

Received:  
13 November 2020

Revised:  
08 January 2021

Accepted:  
12 January 2021

© 2021 The Authors. Published by the British Institute of Radiology under the terms of the Creative Commons Attribution-NonCommercial 4.0 Unported License <http://creativecommons.org/licenses/by-nc/4.0/>, which permits unrestricted non-commercial reuse, provided the original author and source are credited.

Cite this article as:

Smith J, Zawaideh JP, Sahin H, Freeman S, Bolton H, Addley HC. Differentiating uterine sarcoma from leiomyoma: BET<sup>1</sup>T<sup>2</sup>ER Check! *Br J Radiol* 2021; **94**: 20201332.

## FEMALE GENITOURINARY ONCOLOGY SPECIAL FEATURE: REVIEW ARTICLE

# Differentiating uterine sarcoma from leiomyoma: BET<sup>1</sup>T<sup>2</sup>ER Check!

<sup>1</sup>JANETTE SMITH, PhD, MRCS, FRCR, <sup>1</sup>JERIES PAOLO ZAWAIDEH, MD, <sup>1</sup>HILAL SAHIN, MD, <sup>1</sup>SUSAN FREEMAN, MRCP, FRCR, <sup>2</sup>HELEN BOLTON, DLM, PhD, MRCOG and <sup>1</sup>HELEN CLARE ADDLEY, MRCP, FRCR

<sup>1</sup>Department of Radiology, Cambridge University Hospitals NHS Foundation Trust, Cambridge, UK

<sup>2</sup>Department of Gynaecological Oncology, Cambridge University Hospitals NHS Foundation Trust, Cambridge, UK

Address correspondence to: Helen Clare Addley  
E-mail: [helenclare.addley@addenbrookes.nhs.uk](mailto:helenclare.addley@addenbrookes.nhs.uk)

### ABSTRACT

Although rare, uterine sarcoma is a diagnosis that no one wants to miss. Often benign leiomyomas (fibroids) and uterine sarcomas can be differentiated due to the typical low T2 signal intensity contents and well-defined appearances of benign leiomyomas compared to the suspicious appearances of sarcomas presenting as large uterine masses with irregular outlines and intermediate T2 signal intensity together with possible features of secondary spread. The problem is when these benign lesions are atypical causing suspicious imaging features. This article provides a review of the current literature on imaging features of atypical fibroids and uterine sarcomas with an aide-memoire BET<sup>1</sup>T<sup>2</sup>ER Check! to help identify key features more suggestive of a uterine sarcoma.

### INTRODUCTION

Uterine leiomyosarcomas are rare compared to leiomyomas, but it can be very difficult to tell these two entities apart. Clinical manifestations of uterine sarcomas and leiomyomas are similar, with increased uterine size, abdominal pain and per vaginal bleeding.<sup>1</sup> Imaging therefore is crucial to be able to differentiate between these diagnoses as benign leiomyomas are amenable to conservative or benign intervention such as uterine fibroid embolisation or limited surgical resections, whereas the malignant sarcomas have a poor prognosis and early complete surgical removal is the optimal treatment to reduce future morbidity and mortality. Benign leiomyomas may have varied appearances on MR imaging with a significant proportion undergoing cystic or haemorrhagic degeneration or being highly cellular in appearance. The differing imaging features therefore provide a challenging imaging diagnostic environment where the stakes are high.

Overcalling of atypical leiomyomas as malignant entities will mean extensive surgery with uterine loss which may otherwise have been treated with less extensive surgery or a non-surgical approach. Conversely, undercalling a potential sarcoma results in delayed diagnosis and inappropriate management with potentially devastating consequences

due to the aggressive nature of these lesions to metastasize, and therefore loss of the opportunity for intervention at the time of uterine limited disease. The subject is a topic of extensive research into the distinguishing MR imaging features which are discussed herein.

#### Imaging of leiomyomas vs uterine sarcomas

Ultrasound and CT do not have the soft tissue discrimination to aid diagnosis between uterine leiomyomas and sarcomas. Features of metastatic spread allow for easy distinction between benign and malignant lesions but are not always present or imaged at the time of initial concern. Metastatic disease is readily diagnosable on ultrasound and CT depending upon the site such as ascites, liver, lung or bone lesions or peritoneal deposits.

MRI is the best imaging modality for assessment of distinguishing features of leiomyomas from uterine sarcomas due to its ability to assess signal intensity of tissue with typical fibroid appearances of a whorled homogeneous low T<sub>2</sub> weighted (T<sub>2</sub>WI) signal intensity (SI) lesion having a very high negative predictive value for a benign fibroid.<sup>2</sup> The European Society of Urogenital Radiology (ESUR)<sup>3</sup> guidelines provide a good rationale for basic and optional MRI sequences (Table 1). These sequences allow for assessment of

Table 1. MRI sequences – ESUR guidelines<sup>3</sup>

Sequence	Plane	Rationale
T2 Pelvis	Axial, Sagittal, and Coronal (optional) and axial oblique to uterus	Anatomy and characterisation
T1 Pelvis	Axial	Lymph node assessment and identify fat or haemorrhage within lesion
T1 Fat saturated pelvis	Axial	Identify fat or haemorrhage within lesion
T2	Fast axial of upper abdomen	Assessment of upper abdominal viscera and lymph nodes
DWI	Axial	Characterise atypical leiomyomas/sarcomas
ADC	Axial	Characterise atypical leiomyomas/sarcomas
Post-gadolinium T1 (optimally DCE)	Best plane for characterisation	Characterise of leiomyomas/sarcomas

ADC, apparent diffusion coefficient; DCE, dynamic contrast-enhanced; DWI, diffusion-weighted imaging.

SI, shape, outline of the lesion and disruption of boundaries such as the serosal and endometrial interfaces which are all helpful in characterising a suspicious lesion for malignancy compared to a benign fibroid. We propose an aide memoire in this article to aid the reading in assessing these features: BET<sup>1</sup>T<sup>2</sup>ER Check:

#### Key features to identify sarcomas – BET<sup>1</sup>T<sup>2</sup>ER Check!

Given the low incidence of uterine sarcoma, there are limited comparable large-scale studies which have evaluated MRI features in leiomyomas and uterine sarcomas, such as leiomyosarcoma (LMS). However, many small cohort studies have repeatedly highlighted several key features which can aid uterine sarcoma detection. The acronym BET<sup>1</sup>T<sup>2</sup>ER check can be used as an aide-memoire. Summary (Table 2) demonstrates key imaging features of uterine sarcomas and atypical leiomyomas.

#### B: Borders

An irregular or poorly defined border is a key suspicious feature (Figure 1) with a high incidence in sarcomas (80.6%–100%) compared to a very low incidence (3.8%) in atypical leiomyomas.<sup>4</sup> In one of the largest studies involving 19 LMS, this feature on MRI gave a 74–84% sensitivity and 86–91% specificity for LMS<sup>5</sup> (Figures 2 and 3).

#### E: Enhancement

The addition of intravenous contrast medium increases the diagnostic accuracy of uterine sarcomas.<sup>6</sup> Myometrially based uterine sarcomas typically demonstrate heterogenous enhancement with irregular, often central, areas lacking contrast enhancement due to necrosis.<sup>5,7,8</sup> This sign is seen in the majority of cases of LMS (80%).<sup>9</sup> Lakhman et al<sup>5</sup> reported that central unenhanced areas on MRI gave a 95–100% sensitivity and 68–73% specificity for LMS (Figure 4).

Table 2. Summary of typical MRI imaging features for leiomyomas and sarcoma: BET<sup>1</sup>T<sup>2</sup>ER Check!

	Typical leiomyoma	Hyaline & cystic degeneration	Red degeneration	Lipo-leiomyoma	Cellular leiomyoma	Sarcoma
Border	Well defined	Well defined	Well defined	Well defined	Well defined	Lobulated or irregular
Enhancement	Heterogeneous	Heterogeneous with no enhancement in degeneration	Heterogeneous with no enhancement in degeneration	Heterogeneous	Homogeneous	Heterogeneous – with irregular outline/ invasion
T1WI SI	Low	Low	Haemorrhage high	Fat high with saturation on fat saturated T1WI	Low	Low with high SI in areas of haemorrhage
T2WI SI	Low	High in cystic areas	Variable depending on age of haemorrhage	Variable given the fat containing component	Intermediate	Intermediate and heterogenous
Endometrial thickening	None	None	None	None	None	Direct involvement/ irregular or thickened
Restricted diffusion	No	No	No	No	Yes	Yes

Figure 1. Sagittal  $T_2W$  MRI of a spindle cell leiomyosarcoma demonstrating aggressive features such as a heterogenous  $T_2W$  intrauterine lesion, irregular border extending through the uterine serosa (white arrows) and additional separate extra uterine peritoneal deposit (\*).



Degenerating leiomyomas also show areas without enhancement corresponding to the areas of degeneration. It is therefore vital that the signal intensity within these areas is compared to the standard  $T_1$  weighted imaging ( $T_1WI$ ) and  $T_2$  weighted imaging ( $T_2WI$ ) to characterise areas of hyaline, cystic or red cell degeneration which have typical signal intensities. In addition, uterine sarcomas demonstrate different enhancement characteristics to leiomyomas with sarcomas demonstrating increased mean contrast enhancement and early enhancement ratios compared to leiomyomas.<sup>4</sup> This is a helpful defining characteristic which can be analysed using dynamic enhancement curves with an enhancement curve Type III with increased mean contrast enhancement and early contrast enhancement ratios in sarcomas compared to leiomyomas.<sup>4</sup>

**T1:  $T_1$  weighted imaging – presence of haemorrhage**  
Subacute haemorrhage produces methaemoglobin, which demonstrates high  $T_1WI$  SI (Figures 2b, e, 3 and 4). This represents haemorrhagic necrosis and is seen in 18–94% of uterine sarcomas<sup>10, 11</sup> compared with 1.3–18% of leiomyomas.<sup>5,12</sup> Intralesional haemorrhage has a high sensitivity (95–100%) and specificity (82–95%) for LMS<sup>5</sup> (Figure 3). In a systematic review of nine studies, intralesional haemorrhage carried a 7.38 times increased risk of LMS compared to a benign lesion.<sup>13</sup> Identification of blood products within the lesion is therefore very helpful for characterisation of sarcoma and is very unusual within a fibroid. An additional factor that helps in characterisation is that when haemorrhage does occur in a fibroid, it is usually due to a

Figure 2. Axial T2 (a) and T1 fat saturated image without (b) and with gadolinium contrast medium (c) MRI of a low grade ESS. The ESS demonstrates myometrial invasion with irregular nodular borders (a, white arrows), heterogenous T2 signal, intralesional haemorrhage (b, black \*), and central poor enhancement (c, white \*). Axial  $T_2W$  (d), axial T1 fat saturated image (e) and DWI (f) MRI of a uterine adenosarcoma. The adenosarcoma demonstrates myometrial invasion with irregular borders (d, white arrows), heterogenous T2 signal, intralesional haemorrhage (e, black \*), and restricted diffusion. (f). ADC maps not shown. ADC, apparent diffusioncoefficient; DWI, diffusion-weighted imaging; ESS, endometrial stromal sarcoma.

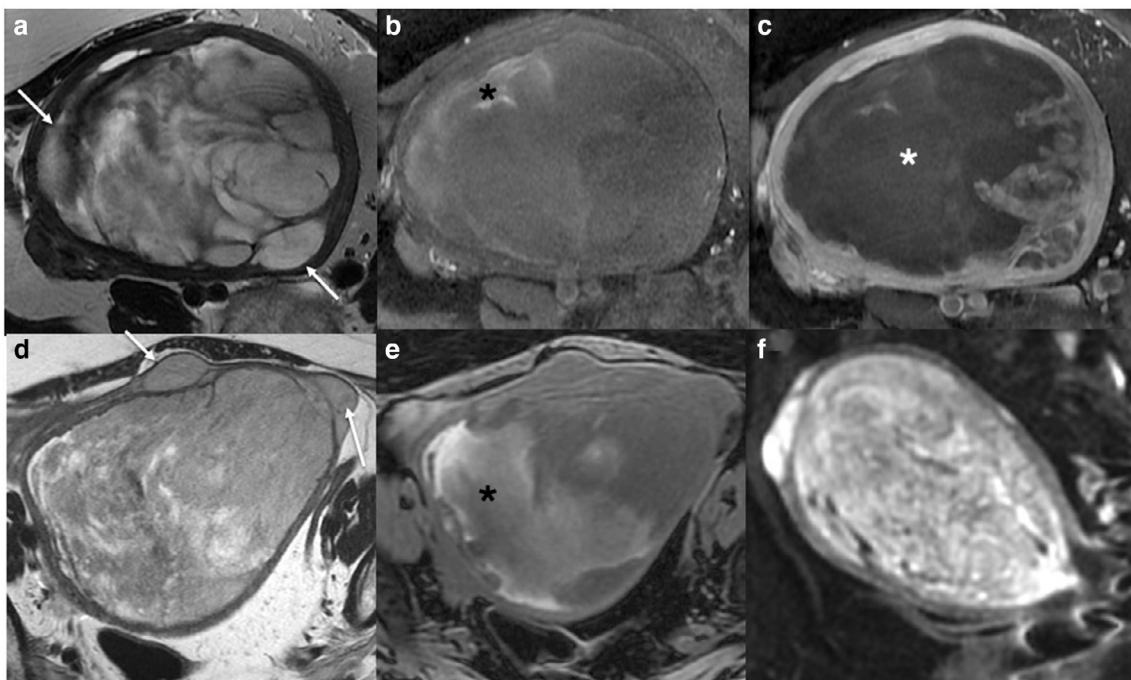
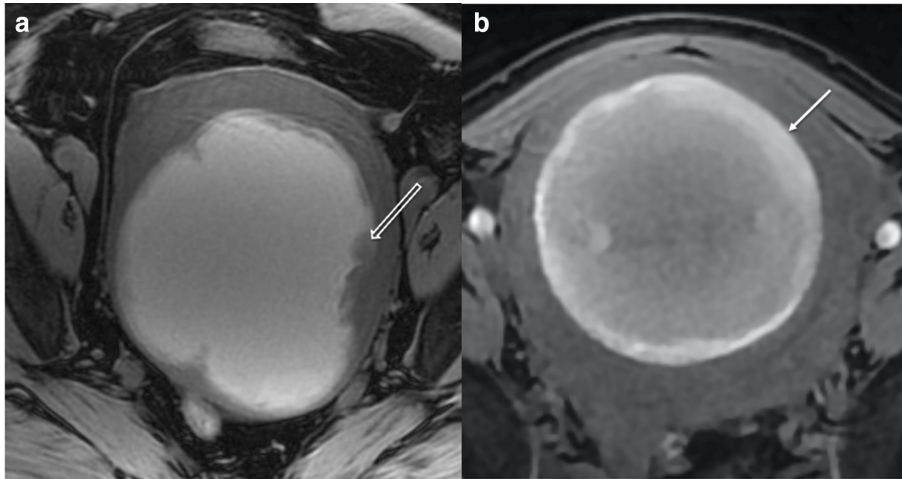


Figure 3. Comparison of imaging in LMS (a) and red cell degeneration of benign fibroid (b): Axial  $T_1W$  fat saturated MRI of two intrauterine lesions. Lesion (a) has diffuse hyperintense  $T_1W$  fat saturated signal with an irregular intermediate T1 signal border and soft tissue projecting into the lesion (open white arrow). Lesion (b) has an intermediate to high  $T_1W$  fat saturated signal intensity with a hyperintense smooth rim and clear distinction of the margin with no internal projections (closed white arrow) in a 40-year-old lady. Surgical histology of lesion (a) confirmed LMS. Lesion (b) had been imaged with MRI 12 months previously, when it had low  $T_2W$  signal. Between the two MRIs, the female had become pregnant and given birth and the follow-up MRI was for further management of her benign leiomyoma, which had undergone red degeneration during pregnancy. LMS, leiomyosarcoma.



typical hormonal insult such as pregnancy or oral contraceptive use and the patient typically presents with an expected history of pain and systemic upset such as fever and leucocytosis. This occurrence is called red cell or carneous degeneration. If imaging is required in pregnancy to confirm diagnosis and exclude differential causes of fever and pain such as appendicitis, then the diagnosis can be made on  $T_1WI$  and  $T_2WI$  alone without the addition of intravenous contrast medium.

The presence of haemorrhage within a uterine mass in the absence of the clinical scenario compatible with red cell degeneration of a fibroid is therefore highly suggestive of a sarcoma. However, acute or chronic haemorrhage may not always be identified. Susceptibility-weighted imaging (SWI) or susceptibility weight angiography (SWAN) can detect deoxyhaemoglobin and haemosiderin and detect areas of previous haemorrhage. In a recent, but small study, low signal on SWAN sequences were detected in

Figure 4. Axial  $T_1W$  fat saturated image without (a) and with (b) gadolinium contrast medium. (a) demonstrates high T1 fat sat signal intensity in keeping with intralesional haemorrhage. Central unenhanced areas are seen in (b) in keeping with a high grade sarcoma (confirmed on histology).

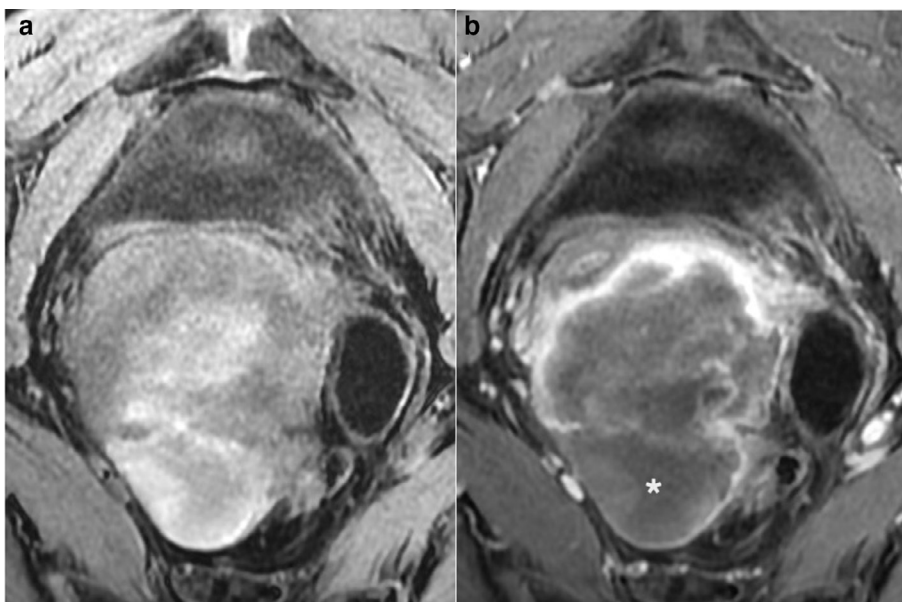
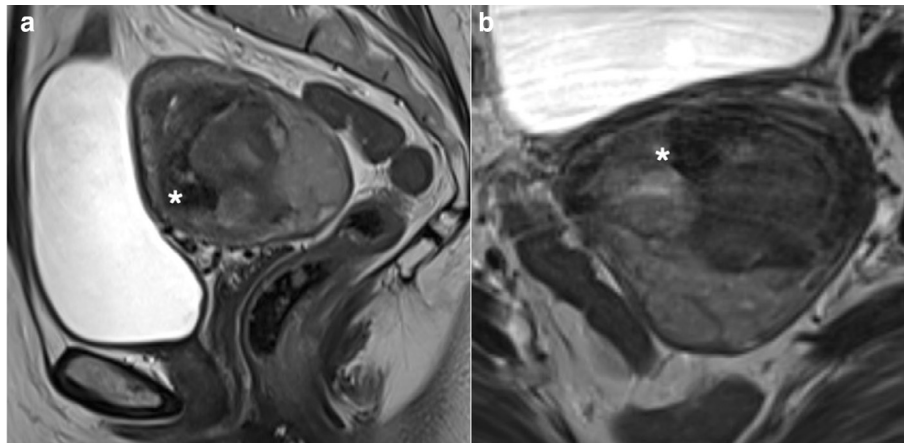


Figure 5. Sagittal (a) and axial (b)  $T_2$ W MRI of a high grade leiomyosarcoma demonstrating heterogenous  $T_2$  signal intensity with focal hypointense  $T_2$  areas (\*) in keeping with haemosiderin within the intrauterine lesion.



100% of uterine sarcomas compared to only 4% of leiomyomas (sensitivity 100% specificity 96%).<sup>14</sup> However, SWI may be too sensitive to haemorrhage as other studies have produced similar results in leiomyomas with red degeneration.<sup>14</sup> Other benign conditions such as adenomyosis can produce multiple small foci of signal voids, which is a pitfall.

#### T2: $T_2$ weighted imaging – low $T_2$ signal intensity dark areas

Low  $T_2$  signal intensity dark areas can be caused by flow voids or intralésion haemosiderin. Lakhman *et al*<sup>5</sup> demonstrated good sensitivity (79–84%) and specificity (86%) for this feature in the diagnosis of LMS (Figure 5). It is unclear if this is an unrecognised or unreported feature,<sup>13</sup> as a recent systematic review identified only 4% reported incidence for LMS with low  $T_2$  signal areas. These features should not be confused with normal low  $T_2$  signal seen in benign leiomyomas and, correlation with  $T_1$ WI and enhancement is helpful.

High  $T_2$  signal intensity has been reported by many groups,<sup>8,13,15</sup> but there can be considerable overlap with degenerating leiomyomas. A high  $T_2$  signal or  $T_2$  heterogeneity was not found to

be significant in Lakhman *et al*'s study.<sup>5</sup> In summary, the signal intensity on  $T_2$ WI in sarcomas is variable as it depends upon the areas of necrosis, soft tissue, flow voids and haemosiderin.

#### E: Endometrial involvement

Adenosarcomas and ESS have a high propensity for endometrial involvement, the aggressive nature of LMS, means that although it originates within the myometrium it can also involve the endometrium in up to 35–50% of cases,<sup>16,17</sup> resulting in loss or irregularity of the endometrial stripe (Figure 6). The outline of the lesion with the endometrium is therefore vital to assess as is the serosal surface for the same reason in cases suspicious for LMS.

#### R: Restricted diffusion

High diffusion-weighted imaging (DWI) SI ( $b = 800\text{--}1000\text{ s mm}^{-2}$ ), greater than that of endometrium, and low ADC values (cut-off value:  $0.79\text{--}1.27 \times 10^{-3} \text{ mm}^2 \text{ s}^{-1}$ )<sup>4,7,18–20</sup> have been found in LMS (Figure 7). However, the routine use of ADC value on its own is limited due to overlap with cellular leiomyoma values<sup>2,4,19,21–24</sup> Figure 7. Different cut-off values have been suggested. These cut-off values range between 0.79 and  $1.27 \times$

Figure 6. Axial  $T_2$ W (a) and axial  $T_1$  fat saturated gadolinium contrast medium enhanced (b) MRI of a high grade leiomyosarcoma demonstrating endometrial invasion (\*) by a leiomyosarcoma (arrows).

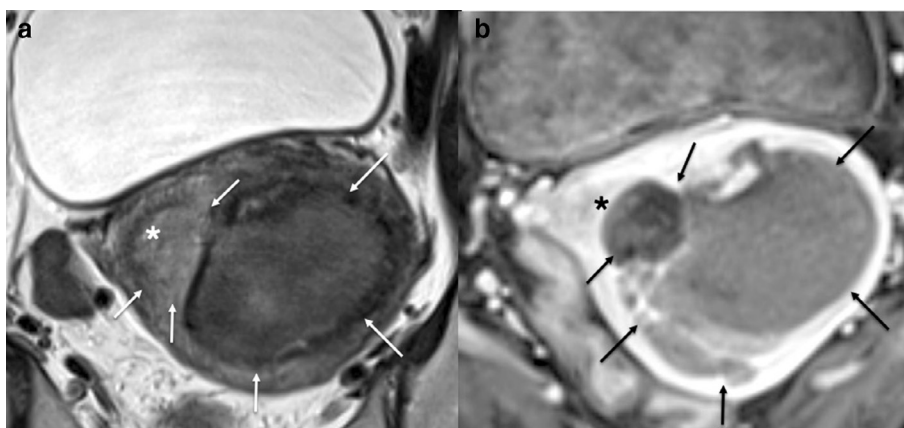
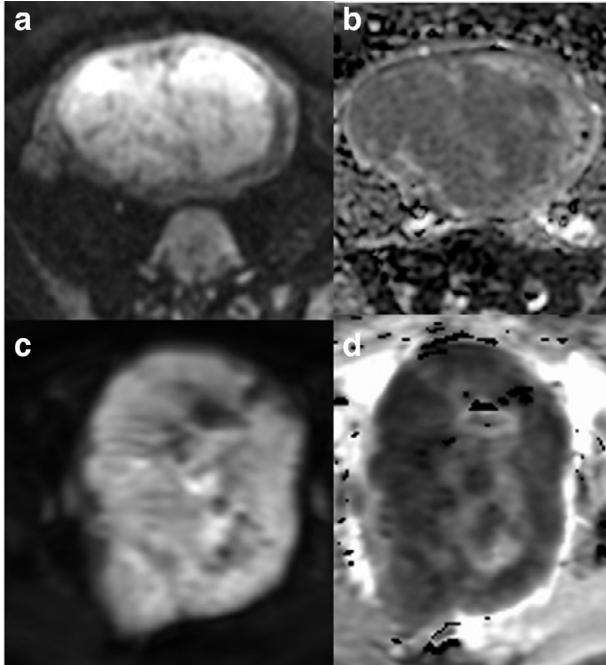


Figure 7. Comparison of DWI imaging in benign (a, b) and malignant (c, d) lesions: axial DWI (a) and ADC (b) of a highly cellular leiomyoma and axial DWI (c) and ADC (d) of a leiomyosarcoma. The DWI outline is helpful in demonstrating the irregular outline in the malignant lesion (c, d). ADC, apparent diffusion coefficient; DWI, diffusion-weighted imaging.



$10^{-3} \text{ mm}^2 \text{ s}^{-1}$ <sup>14,7,18-20</sup> and may be due to different MRI machines, field strengths and study design.

In terms of benign lesions, Wahab et al<sup>18</sup> found that in cases where the DWI SI of the lesion was less than that of myometrium or greater than myometrium but less than that of endometrium or lymph nodes, then the lesion was almost certainly benign and conversely a DWI SI greater than endometrium and an ADC value less than or equal to  $0.905 \times 10^{-3} \text{ mm}^2 \text{ s}^{-1}$  had a high prediction for malignancy.

An important pitfall to be aware of is the misinterpretation of restricted DWI in areas of blood products and therefore the misinterpretation of benign red cell degeneration. Correlation of restricted DWI areas on both  $T_2$  and  $T_1$ WI is therefore mandatory in interpretation of DWI findings.

### Leiomyomas

Leiomyomas, or fibroids, are the most common benign uterine tumour with 20–80% of pre-menopausal females affected,<sup>3,24,25</sup> although not all will have symptoms. Leiomyomas are comprised of smooth muscle tissue and excess extracellular fibrous supporting tissue and are under the hormonal influence of oestrogen and progesterone. They can occur at variety of different sites throughout the myometrium, such as subserosal, intramural and submucosal locations. During reproductive years, especially during pregnancy, leiomyomas can increase in size and typically reduce during post-menopausal period. Risk factors for leiomyomas can be found in Table 3. There is conflicting evidence on

Table 3. Risk factors for leiomyomas

Risk factors for leiomyomas	
Race	African ancestors > other races
Genetic	e.g. hereditary leiomyomatosis and renal cell carcinoma
Diet	High consumption of red meat Reduced intake of vegetables, fruit and vitamin D
Gynaecology history	Multiparity, polycystic ovarian syndrome, hormone replacement therapy

the effect of oral contraceptive on the development and growth of leiomyomas.

There are many options for treatment of fibroids, but it is important when reporting the imaging to recognise that in addition to medical and interventional radiology options the standard surgical options also now conserve the uterus.<sup>26</sup> Laparoscopic or hysteroscopic myomectomy (often requiring morcellation), uterine artery embolisation (UAE), and high intensity focus ultrasound mean that the uterus remains *in situ*. Thus, an unexpected pre-operative uterine sarcoma may be spread throughout the abdominal cavity with techniques such as power morcellation, resulting in increased risk of recurrence and reduced survival.<sup>27-29</sup> Because of this, the United States Food and Drug Administration issued a warning in 2014<sup>30</sup> and European Society of Gynaecological Endoscopy published a position statement in 2016<sup>31</sup> regarding worsening outcomes in patients with unsuspected uterine sarcomas who underwent leiomyoma morcellation. Limited studies suggest that UAE does not appear to cause dissemination but is strongly advised against if there is any concern about LMS as it delays appropriate treatment for LMS.<sup>32</sup>

### Typical leiomyoma imaging features

On MRI, these include low  $T_2$ WI lesions with a slightly whorled appearance, well-defined borders with no invasion. Enhancement often follows that of myometrium. They can be located throughout the myometrium in a subserosal, intramural or submucosal distribution, with the FIGO PALM-COEIN classification Figure 8<sup>33</sup>

Atypical leiomyomas may have several histological features which can be easily recognised on MR imaging:

- Oedema

Peripheral or diffuse heterogenous high  $T_2$ WI on the background of low  $T_2$ WI signal intensity with normal enhancement may indicate oedema. This may be the first sign of degeneration.<sup>9</sup>

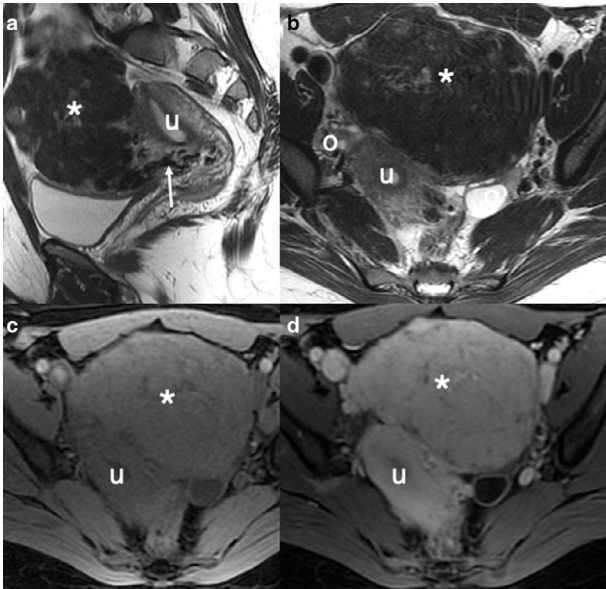
- Degeneration

Degeneration tends to occur in leiomyomas >5 cm and can be:

- (i) Hyaline (60%)

MRI characteristics may not change significantly, as the collagen deposited in hyaline degeneration is usually low

Figure 8. Typical benign fibroid: sagittal (a) and axial (b)  $T_2$ W images demonstrating a well-defined low SI mass (\*) extending anteriorly from the uterus (u) and separate to the ovaries (o) with bridging vessels (white arrow) in keeping with a sub-serosal fibroid. The 'whorled' and low  $T_2$ WI SI is typical for benign fibroid. Axial  $T_1$ W images before (c) and following (d) the administration of intravenous contrast medium demonstrates intense enhancement of the fibroid with no necrosis.



signal intensity on T2 and intermediate on  $T_1$ WI. Very little or no contrast enhancement will be seen within hyaline areas<sup>9</sup> due to the accumulation of proteinaceous material in the extracellular space preventing gadolinium entering.

(ii) Cystic (4%)

This is characterised by high  $T_2$  and low  $T_1$ WI spaces with a thin low T2 signal rim and associated enhancement, representing residual leiomyoma tissue.<sup>9,34</sup>

(iii) Myxoid (uncommon)

This is due to myxoid matrix and extracellular mucin deposition and demonstrates high T2 and low T1 signal intensity but with contrast medium enhancement.<sup>9</sup>

(iv) Red/haemorrhagic or carneous (Figure 3)

This occurs in leiomyomas during pregnancy or with oral contraceptive use.<sup>34</sup> Torted fibroids may also become ischaemic and haemorrhagic. Peripheral or diffuse high T1 signal intensity is seen, with corresponding low T2 signal due to blood degradation products. There is no contrast enhancement.<sup>9</sup>

Other atypical leiomyomas may present with a different spectrum of signal intensities. These include:

- Cellular leiomyoma (Figure 7a) (Rare)

They are typically well-defined and mildly hyperintense on  $T_2$ WI due to high cellularity, with homogenous contrast enhancement. Due to their high cellularity, these leiomyomas often demonstrate restricted diffusion.<sup>34</sup>

- Lipoleiomyoma (Figure 9)

These are rare leiomyomas containing mature macroscopic fat. High T1 signal intensity within the leiomyoma, which suppresses on fat suppressed sequences is characteristic. Fat attenuation can be seen on CT. Some lipoleiomyomas contain microscopic fat which can only be detected on in-and-out of phase sequences.<sup>34</sup> The appearance of fat is regarded as characteristic for lipoleiomyoma as liposarcoma arising within the uterus is extremely rare.

- Intravascular leiomyomas (Figure 10)

This rare condition is characterised by aggressive intravenous growth of a leiomyoma. The involved veins may be intra- or extrauterine and include major veins of the pelvis and abdomen (Figure 10). In 10–40%, the heart can be involved.<sup>35–37</sup> MRI characteristics depend on the amount of smooth muscle and fibrous components in the tumour, but characteristically have similar appearances to benign or cellular leiomyomas. Surgical resection and hormone treatment is required.<sup>38</sup>

- Benign metastasising leiomyomas

This rare and unusual condition occurs when benign leiomyomas metastasise to other organs distant from the uterus. Lung metastases are most common and are often found incidentally on chest X-ray or imaging for other conditions. The tumours are under hormonal influence and can spontaneously resolve.<sup>39</sup> They can sometimes cavitate and may cause a pneumothorax but rarely

Figure 9. Axial  $T_2$ W (a),  $T_1$ W (b) and  $T_1$ W fat saturated (c) images of a uterine lipoleiomyoma. Axial portal venous contrast-enhanced CT of the pelvis (d) confirms fat attenuation within the uterine lesion.

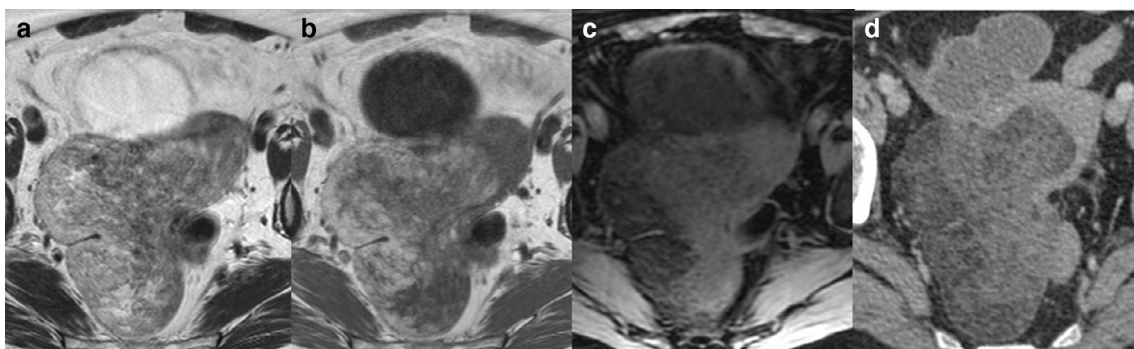
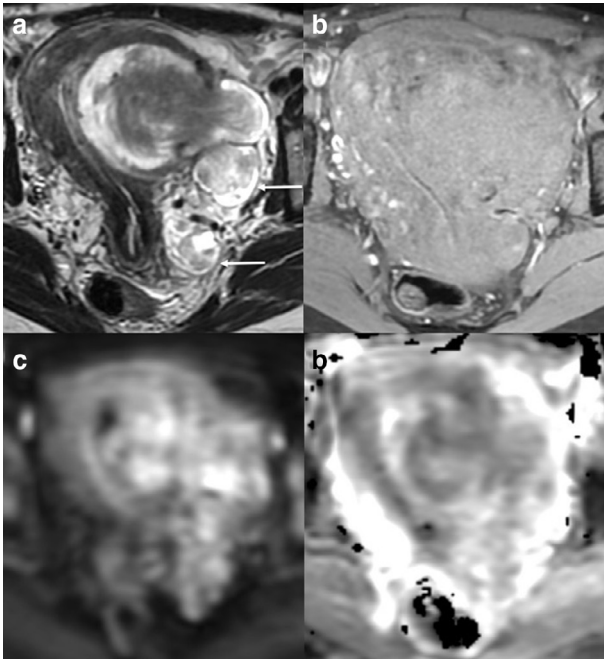


Figure 10. Axial  $T_2W$  (a),  $T_1W$  fat saturated image (b), DWI (c) and ADC (d) of a uterine lesion in a 45-year-old females. Heterogenous  $T_2W$  lesion demonstrates extension through the myometrium with high T2 signal 'deposits' within the left of the pelvis (white arrows). No lymph node enlargement or metastasis was seen on staging CT. Pre-operative diagnosis of a uterine sarcoma was made and a total hysterectomy and bilateral salpingo-oophorectomy performed. Leiomyomatosis with intravascular invasion was confirmed on histology. ADC, apparent diffusion coefficient; DWI, diffusion-weighted imaging.



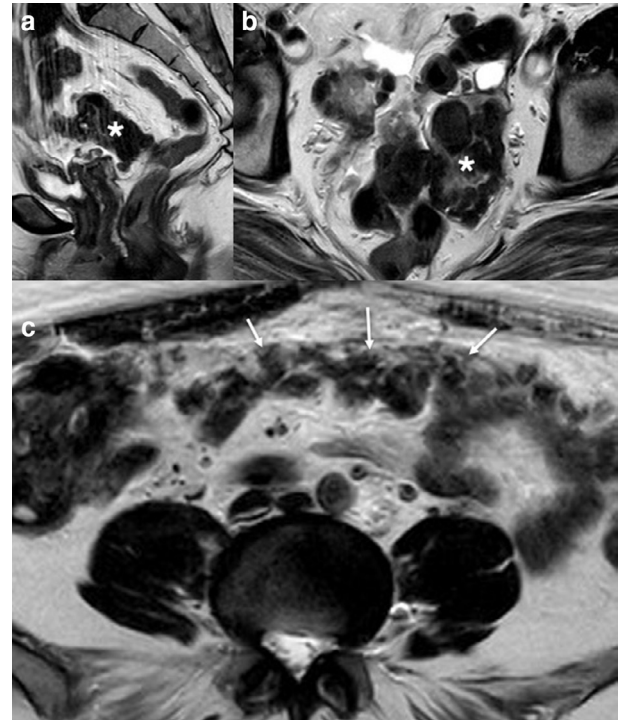
calcify. The metastases are otherwise non-specific on CT or MRI and can mimic malignant metastases, sarcoidosis, amyloidosis and rheumatoid nodules.<sup>40,41</sup> Patients often have a past medical history for treated leiomyomas, such as hysterectomy.

- Parasitic, peritoneal and retroperitoneal leiomyomatosis

All these entities are rare but together describe the presence of leiomyomas separate to the uterus in different abdominal and pelvic locations. In parasitic leiomyomas, the leiomyomas originate from the uterus and subsequently develop a blood supply from their surroundings before loosening their attachment with the uterus. Common sites include broad ligament, ovary, bladder, ureter and urethra. They have similar imaging characteristics to benign leiomyoma but can mimic lymphadenopathy or benign or malignant tumours. Broad ligament tumours can be associated with a raised CA125 and pseudo-Meig's syndrome.<sup>42</sup> These leiomyomas can also undergo degenerative changes and developing imaging characteristics similar to atypical leiomyoma within the uterus.<sup>43</sup>

In peritoneal leiomyomatosis, multiple leiomyoma grow within the abdominal cavity on the peritoneum and omentum typically from seeding from previous surgery (Figure 11). It is often identified incidentally and is associated with increased levels of

Figure 11. Sagittal (a) and axial (b)  $T_2W$  images demonstrating previous hysterectomy (for fibroids) with a well-defined low signal intensity mass (\*). Axial  $T_2W$  (c) image of the abdomen demonstrates low signal intensity mass outlining the peritoneum (white arrows). This had been mistaken for an ovarian Stage 3C malignancy on CT imaging but the CA-125 level was normal. Biopsy of the peritoneal area confirmed peritoneal leiomyomatosis.



progesterone and oestrogen such as pregnancy, oral contraceptive use and oestrogen-producing tumours such as granulosa cell tumours.<sup>40</sup> Rounded nodules can be seen throughout the peritoneal cavity which have the same signal characteristics as muscle on MRI. Abdominal appearances can mimic peritoneal or ovarian carcinoma, mesothelioma, dermoid tumours and tuberculosis.<sup>40</sup>

Retroperitoneal leiomyomatosis is often found incidentally and given the location in the retroperitoneum can mimic other retroperitoneal pathology including lymphoma.<sup>40</sup>

- Smooth muscle tumours of uncertain malignant potential (STUMP) (Figure 12)

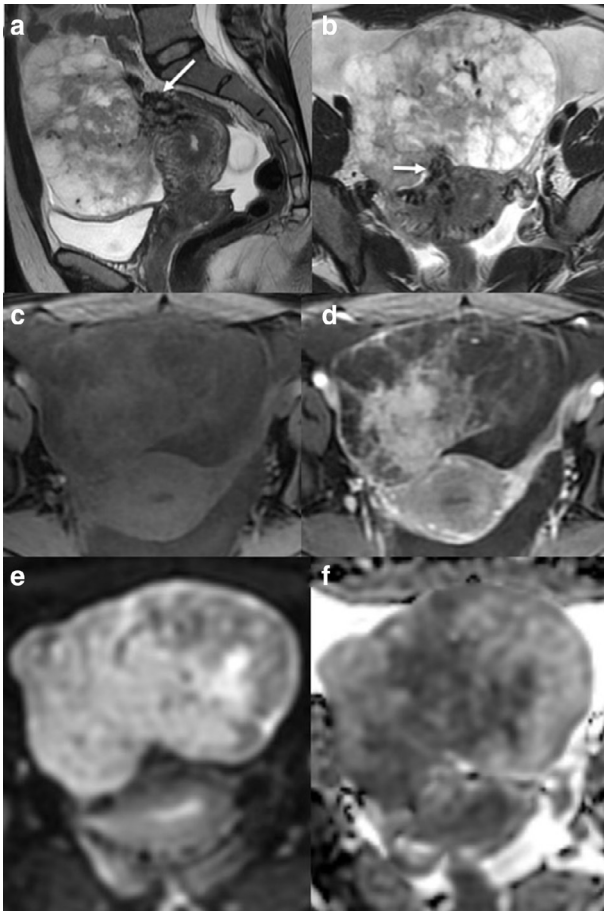
These are rare tumours with some concerning features on pathology (in addition to imaging), such as nuclear atypia, necrosis and mitotic figures, but cannot be formally classified as malignant. They therefore represent a separate category according to pathological diagnosis and not surprisingly, they have a variety of MRI appearances from typical benign leiomyoma appearances to a classical leiomyosarcoma appearances.<sup>9</sup>

### Uterine sarcomas

Uterine sarcomas are uncommon making up 1% of all gynaecological tract and 8% of all uterine malignancies.<sup>1,24,44</sup> Of uterine



Figure 12. Sagittal (a) and axial (b)  $T_2W$  images of an exophytic uterine lesion with a narrow base. The lesion demonstrates bridging vessels (White arrow) and cystic peripheral changes. The central area of enhancement and peripheral poor enhancement is seen on the T1 fat saturated imaging without (c) and with gadolinium contrast medium (d). DWI (e) and ADC (f) demonstrate central restricted diffusion within the lesion. Pre-operatively imaging suggested a tortured large subserosal leiomyoma. However, on histology, a smooth muscle tumour of uncertain malignant potential was diagnosed. ADC, apparent diffusion coefficient; DWI, diffusion-weighted imaging



sarcomas, LMS is the most common type comprising 70% of cases. LMS are found incidentally in 0.09–0.49% of hysterectomy specimens.<sup>45–47</sup> However, it is important to remember that benign smooth muscle tumours of the uterus are extremely common and only about 1/1000 uterine smooth muscle tumours are sarcomas.

Risk factors for leiomyosarcomas and other uterine sarcomas are not well understood (Table 4). Older age at menarche (*i.e.* menarche at >15 years vs <11 years) and tubal ligation are protective.<sup>49</sup>

#### (a) Leiomyosarcoma (Figure 1)

- The majority of LMS arise *de-novo* within the myometrium with only 0.2% arising within a pre-existing leiomyoma.<sup>48,50,51</sup>

Table 4. Risk factors for uterine sarcoma<sup>48</sup>

Risk factors for Uterine sarcomas	
Age	>40 years
Obesity	>30 kg m <sup>-2</sup> vs <25 kg m <sup>-2</sup>
Other medical conditions	Diabetes, previous radiotherapy, long term tamoxifen use

Molecular studies have demonstrated differences in micro-RNA expression and biomarkers between leiomyomas and LMS suggesting separate aetiologies and developmental pathways.<sup>52,53</sup> Although LMS can invade into the endometrium, pre-operative endometrial biopsy has been shown to only detect approximately 35–50% of cases.<sup>16,17</sup>

#### (b) Endometrial stromal sarcomas (Figure 2a–c)

- These account for 10–15% of uterine sarcomas and can be divided into low (LGESS) and high grade (HGESS).<sup>51</sup> Younger females (average 39 years) tend to be diagnosed with LGESS while post-menopausal females (average 61 years) more commonly have HGESS. LGESS has a good prognosis and can have a worm like or nodular appearance on MRI as the tumour extends through the myometrium and serosa<sup>54</sup> (Figure 2a–c).

#### (c) Undifferentiated sarcomas

- These sarcomas have a poor prognosis, especially if vascular invasion or haematological spread are present. They are often endometrial in location and can be detected on pre-operative endometrial biopsy.

#### (d) Adenosarcomas (Figure 2d–f)

- These are rare slow-growing uterine sarcomas which account for 5.5–9% of all uterine sarcomas.<sup>55</sup> They are composed of malignant sarcomatous elements and benign glandular tissue and tend to occur within the endometrial cavity in 70% of cases. Myometrial, cervical and ovarian locations have also been described, and are more commonly seen in younger patients.<sup>55,56</sup> Sarcomatous overgrowth (>25%) can occur which results in poorer prognosis. Myometrial and lymphovascular invasion are further poor prognostic signs, with 33% recurring within 5 years of diagnosis.

#### (e) Carcinosarcoma

- Carcinosarcomas have recently been reclassified as an aggressive form of endometrial carcinoma<sup>57</sup> rather than true uterine sarcoma. They have both sarcomatous and carcinoma elements, which include endometrioid, serous, squamous, adenocarcinoma or a mix of different types.

#### Typical uterine sarcoma MR imaging features

A typical LMS will present as a large tumour with irregular borders, areas of intralesion haemorrhage, necrosis and early central enhancement in the soft tissue part of the tumour at 40–60 s post-i.v. contrast medium administration.<sup>6</sup> In some cases, extrauterine spread is seen, including ascites and peritoneal

deposits<sup>18,21,58</sup> (Figure 1). Other types of uterine sarcoma have slightly different appearances.

ESS tend to form heterogenous high T2 and low T1 signal intensity polypoid masses within the endometrial cavity, with 'bag of worms' appearance from serpiginous high T2 SI tumour spreading along and compressing smooth muscle fibres.<sup>21,58,59</sup> Necrosis, and haemorrhage are also features in ESS as in LMS (Figure 2a–c). Contrast enhancement of these tumours is often heterogenous, iso- or hyperintense compared to the myometrium, whilst endometrial cancer often demonstrates hypoenhancement compared to the myometrium.<sup>48,59</sup>

Adenosarcomas are also large polypoid masses within the endometrial cavity (Figure 2d–f), causing it to expand and tumour can prolapse through the cervical canal. These tumours can have both glandular cystic spaces or necrosis, producing high T2 signal intense foci and can mimic trophoblastic disease. The polypoid 'lacelike' appearance in addition to the solid components can also be confused with a benign polyp but the heterogeneity is helpful in distinguishing. Solid components will enhance with contrast medium. Myometrial invasion, haemorrhage and necrosis can occur with sarcomatous overgrowth. On DWI high b values, adenosarcomas can show low signal intensity, which is an indication of their low grade.<sup>51,60,61</sup> Unenhanced regions can also be seen in carcinosarcomas, and although this in itself is not a poor prognostic sign, when necrosis comprises  $\geq 10\%$  of the total tumour, it is correlated with poor prognosis.<sup>62</sup>

#### Combining features and algorithms

Although some of the features described in BET<sup>1</sup>T<sup>2</sup>ER check give a high sensitivity and specificity for uterine sarcomas, especially LMS, there is still overlap with atypical leiomyomas. Combining features improves the sensitivity, specificity and accuracy for the diagnosis of uterine sarcoma.

Most studies are small and have identified different imaging or clinical features to differentiate uterine sarcomas from leiomyomas.

Lakhman et al<sup>5</sup>, whose study with 19 confirmed LMS and 22 atypical leiomyomas, demonstrated increased specificity and sensitivity for LMS of 95–100% when 3 or more of the following MRI features were identified; irregular borders, T1 hyperintense signal, T2 dark areas and central unenhanced areas.

Similarly, Thomassin-Naggara et al<sup>2</sup>'s study of 25 uncertain or malignant sarcomas and 26 leiomyomas identified that high DWI b1000 signal intensity, mean ADC value of  $<1.23 \times 10^{-3} \text{ mm}^2 \text{ s}^{-1}$  and an intermediate T<sub>2</sub>W signal intensity distinguished 92.4% of uterine sarcoma from benign leiomyomas.

These features are similar to those identified in a large recent case controlled retrospective studies. The development of an algorithm for the presence of lymphadenopathy, DWI signal greater than that of endometrium and low ADC  $\leq 0.095 \times 10^3 \text{ mm}^2 \text{ s}^{-1}$  provided high sensitivities and specificities for experienced (88 and 100%) and less experienced readers (83 and 97%). The

group also demonstrated that the combined features of low T2 signal solid regions (*i.e.* enhancing benign typical fibroid tissue compared to T2 dark area flow voids or haemosiderin in uterine sarcoma), low DWI signal of the myometrial lesion compared to endometrium and no lymph nodes or ascites allowed correct diagnosis of a benign uterine lesion in 100% of their cases.<sup>18</sup>

A simple decision tree developed by machine learning techniques on 84 benign and 21 malignant lesions also demonstrated that predominantly high T<sub>2</sub>WI signal, restricted diffusion and central necrosis as important features with a 100% sensitivity and 95% specificity.<sup>15</sup> This simple decision tree demonstrated that lesions which did not have these features were likely to be benign. Only four benign lesions were misclassified as malignant using the simple algorithm, while none of the malignant lesions were misclassified.

Goto et al<sup>6</sup> suggest combining clinical and biochemical markers with MRI features. They demonstrated improved diagnosis when using contrast enhanced MRI over unenhanced MRI in a study of 10 LMS and 130 leiomyomas with degeneration. They showed that tumour contrast enhancement at 60 s after administration of Gd-DTPA was detected in all LMS, but absent in 28 of 32 of their leiomyoma patients. This feature improved the positive predictive value from 52.6 to 83.3% and their diagnostic accuracy from 93.1 to 95.2%. When they combined contrast enhanced MRI features with serum lactate dehydrogenase measurements, the specificity, PPV and diagnostic accuracy increased to 100%.<sup>6</sup> Patient age  $\geq 44$  years old also demonstrated increased sensitivity (82.4%) and specificity (92.2%) of LMS over leiomyomas.<sup>63</sup> This has led to some centres combining imaging, biochemical and other features such as endometrial biopsy formally or converting open myomectomy procedures when a case is indeterminate pre-operatively. This was evaluated in the study by Nagai et al<sup>64</sup> who used combined imaging, biochemical and pathological pre-operative features in a formal Preoperative Sarcoma Score (PRESS) with an accuracy rate of prediction of sarcoma of 84.1% using this score.

Although many of the MRI features and the use of contrast enhancement has been included in latest European imaging guidelines, the combination with LDH measurements has not been included,<sup>3</sup> which may be because LDH can also be raised in cellular and degenerating leiomyomas.<sup>6</sup>

#### Other techniques and modalities

Lakhman et al<sup>5</sup> used advanced processing texture analysis techniques of regions of interest on the T<sub>2</sub>W images. Using these techniques, they demonstrate increased textural heterogeneity but reduced entropy in LMS compared to atypical leiomyomas. In a further texture analysis study of LMS and leiomyomas, multiple MRI sequences were assessed. Gerges et al<sup>63</sup> demonstrated T2 and T1 solid area texture analysis were most useful while ADC maps analysis was not significantly different between the two lesions. Although this is still a research technique, it suggests that potential computer analysis of current standardised MRI sequences could be used to improve diagnostic accuracy in the future.

Several groups have investigated the use of PET/CT in distinguishing uterine sarcomas from leiomyomas. In a recent small  $^{18}\text{F}$ -FDG-PET/CT study of 34 uterine sarcomas, the SUVmax cut-off <4.4 had a 100% negative predictive value for a uterine sarcoma, and therefore absence of uptake is very helpful in excluding LMS<sup>65</sup> with a high SUVmax being associated with a worse prognosis.<sup>66</sup> However, the specificity of PET/CT is reduced compared to MRI.<sup>67</sup>

3'-deoxy-3'- $^{18}\text{F}$ -fluorothymidine PET (18F-FLT-PET) allows assessment of tumour proliferation without uptake of the tracer agent by inflammatory tissues. It has been shown to be superior to  $^{18}\text{F}$ -FDG-PET/CT in distinguishing uterine sarcomas from leiomyomas and tracer uptake correlates with immunohistochemical indices of cellular proliferation.<sup>68</sup> However, it is not commonly available in routine clinical practice.

## SUMMARY

Although uterine sarcomas are rare, it is vital to raise suspicion on pre-operative imaging to provide timely priority referral for appropriate surgical planning. MRI is the best modality for assessing uterine sarcomas with CT used for assessment of distant spread. Atypical leiomyomas which have undergone degeneration, are cellular, metastasising or intravascular leiomyomas all have at least one key feature that can mimic diagnosis of LMS on MRI but combining MR imaging features and taking into account the clinical scenario are helpful. Identifying these key MR imaging features such as irregular Borders, heterogenous Enhancement with central poor enhancement, hyperintense  $T_1W$  signal in keeping with haemorrhage, T2 dark areas from vascular signal voids and haemosiderin, Endometrial invasion and restricted diffusion together aids successful pre-operative suspicion for sarcoma with the combination increasing sensitivity, specificity and accuracy. These can be remembered as the acronym BET<sup>1</sup>T<sup>2</sup>ER check.

## REFERENCES

1. Wu T-I, Yen T-C, Lai C-H. Clinical presentation and diagnosis of uterine sarcoma, including imaging. *Best Pract Res Clin Obstet Gynaecol* 2011; **25**: 681–9. doi: <https://doi.org/10.1016/j.bpobgyn.2011.07.002>
2. Thomassin-Naggara I, Dechoux S, Bonneau C, Morel A, Rouzier R, Carette M-F, et al. How to differentiate benign from malignant myometrial tumours using MR imaging. *Eur Radiol* 2013; **23**: 2306–14. doi: <https://doi.org/10.1007/s00330-013-2819-9>
3. Kubik-Huch RA, Weston M, Nougaret S, Leonhardt H, Thomassin-Naggara I, Horta M, et al. European Society of urogenital radiology (ESUR) guidelines: MR imaging of leiomyomas. *Eur Radiol* 2018; **28**: 3125–37. doi: <https://doi.org/10.1007/s00330-017-5157-5>
4. Bi Q, Xiao Z, Lv F, Liu Y, Zou C, Shen Y. Utility of clinical parameters and multiparametric MRI as predictive factors for differentiating uterine sarcoma from atypical leiomyoma. *Acad Radiol* 2018; **25**: 993–1002. doi: <https://doi.org/10.1016/j.acra.2018.01.002>
5. Lakhman Y, Veeraraghavan H, Chaim J, Feier D, Goldman DA, Moskowitz CS, et al. Differentiation of uterine leiomyosarcoma from atypical leiomyoma: diagnostic accuracy of qualitative MR imaging features and feasibility of texture analysis. *Eur Radiol* 2017; **27**: 2903–15. doi: <https://doi.org/10.1007/s00330-016-4623-9>
6. Goto A, Takeuchi S, Sugimura K, Maruo T. Usefulness of Gd-DTPA contrast-enhanced dynamic MRI and serum determination of LDH and its isozymes in the differential diagnosis of leiomyosarcoma from degenerated leiomyoma of the uterus. *Int J Gynecol Cancer* 2002; **12**: 354–61. doi: <https://doi.org/10.1046/j.1525-1438.2002.01086.x>
7. Lin G, Yang L-Y, Huang Y-T, Ng K-K, Ng S-H, Ueng S-H, et al. Comparison of the diagnostic accuracy of contrast-enhanced MRI and diffusion-weighted MRI in the differentiation between uterine leiomyosarcoma / smooth muscle tumor with uncertain malignant potential and benign leiomyoma. *J Magn Reson Imaging* 2016; **43**: 333–42. doi: <https://doi.org/10.1002/jmri.24998>
8. Tanaka YO, Nishida M, Tsunoda H, Okamoto Y, Yoshikawa H. Smooth muscle tumors of uncertain malignant potential and leiomyosarcomas of the uterus: Mr findings. *J Magn Reson Imaging* 2004; **20**: 998–1007. doi: <https://doi.org/10.1002/jmri.20207>
9. Bolan C, Caserta MP. Mr imaging of atypical fibroids. *Abdom Radiol* 2016; **41**: 2332–49. doi: <https://doi.org/10.1007/s00261-016-0935-0>
10. Takeuchi M, Matsuzaki K, Harada M. Carcinosarcoma of the uterus: MRI findings including diffusion-weighted imaging and MR spectroscopy. *Acta Radiol* 2016; **57**: 1277–84. doi: <https://doi.org/10.1177/0284185115626475>
11. Takeuchi M, Matsuzaki K, Harada M. Clinical utility of susceptibility-weighted Mr sequence for the evaluation of uterine sarcomas. *Clin Imaging* 2019; **53**: 143–50. doi: <https://doi.org/10.1016/j.clinimag.2018.10.015>
12. Ando T, Kato H, Furui T, Morishige K-I, Goshima S, Matsuo M. Uterine smooth muscle tumours with hyperintense area on  $T_1$  weighted images: differentiation between leiomyosarcomas and leiomyomas. *Br J Radiol* 2018; **91**: 20170767. doi: <https://doi.org/10.1259/bjr.20170767>
13. Kaganov H, Ades A, Fraser DS. Preoperative magnetic resonance imaging diagnostic features of uterine leiomyosarcomas: a systematic review. *Int J Technol Assess Health Care* 2018; **34**: 172–9. doi: <https://doi.org/10.1017/S0266462318000168>
14. Takeuchi M, Matsuzaki K, Bando Y, Harada M. Evaluation of red degeneration of uterine leiomyoma with susceptibility-weighted MR imaging. *Magn Reson Med Sci* 2019; **18**: 158–62. doi: <https://doi.org/10.2463/mrms.mp.2018-0074>
15. Malek M, Tabibian E, Rahimi Dehgolan M, Rahmani M, Akhavan S, Sheikh Hasani S, et al. A diagnostic algorithm using multiparametric MRI to differentiate benign from malignant myometrial tumors: Machine-Learning method. *Sci Rep* 2020; **10**: 7404. doi: <https://doi.org/10.1038/s41598-020-64285-w>
16. Skorstad M, Kent A, Lieng M. Preoperative evaluation in women with uterine leiomyosarcoma. A nationwide cohort study. *Acta Obstet Gynecol Scand* 2016; **95**: 1228–34. doi: <https://doi.org/10.1111/aogs.13008>
17. Peters A, Sadecky AM, Winger DG, Guido RS, Lee TTM, Mansuria SM, et al.

- Characterization and preoperative risk analysis of leiomyosarcomas at a high-volume tertiary care center. *Int J Gynecol Cancer* 2017; **27**: 1183–90. doi: <https://doi.org/10.1097/IGC.0000000000000940>
18. Abdel Wahab C, Jannot A-S, Bonaffini PA, Bourillon C, Cornou C, Lefrère-Belda M-A, et al. Diagnostic algorithm to differentiate benign atypical leiomyomas from malignant uterine sarcomas with diffusion-weighted MRI. *Radiology* 2020; **297**: 361–71. doi: <https://doi.org/10.1148/radiol.2020191658>
  19. Tamai K, Koyama T, Saga T, Morisawa N, Fujimoto K, Mikami Y, et al. The utility of diffusion-weighted MR imaging for differentiating uterine sarcomas from benign leiomyomas. *Eur Radiol* 2008; **18**: 723–30. doi: <https://doi.org/10.1007/s00330-007-0787-7>
  20. Sato K, Yuasa N, Fujita M, Fukushima Y. Clinical application of diffusion-weighted imaging for preoperative differentiation between uterine leiomyoma and leiomyosarcoma. *Am J Obstet Gynecol* 2014; **210**: 368.e1–368.e8. doi: <https://doi.org/10.1016/j.ajog.2013.12.028>
  21. Sahdev A, Sohaib SA, Jacobs I, Shepherd JH, Oram DH, Reznick RH. Mr imaging of uterine sarcomas. *AJR Am J Roentgenol* 2001; **177**: 1307–11. doi: <https://doi.org/10.2214/ajr.177.6.1771307>
  22. Namimoto T, Yamashita Y, Awai K, Nakaura T, Yanaga Y, Hirai T, et al. Combined use of T2-weighted and diffusion-weighted 3-T MR imaging for differentiating uterine sarcomas from benign leiomyomas. *Eur Radiol* 2009; **19**: 2756–64. doi: <https://doi.org/10.1007/s00330-009-1471-x>
  23. Bonneau C, Thomassin-Naggara I, Dechoux S, Cortez A, Darai E, Rouzier R. Value of ultrasonography and magnetic resonance imaging for the characterization of uterine mesenchymal tumors. *Acta Obstet Gynecol Scand* 2014; **93**: 261–8. doi: <https://doi.org/10.1111/aogs.12325>
  24. Sun S, Bonaffini PA, Nougaret S, Fournier L, Dohan A, Chong J, et al. How to differentiate uterine leiomyosarcoma from leiomyoma with imaging. *Diagn Interv Imaging* 2019; **100**: 619–34. doi: <https://doi.org/10.1016/j.diii.2019.07.007>
  25. Pavone D, Clemenza S, Sorbi F, Fambrini M, Petraglia F. Epidemiology and risk factors of uterine fibroids. *Best Pract Res Clin Obstet Gynaecol* 2018; **46**: 3–11. doi: <https://doi.org/10.1016/j.bpobgyn.2017.09.004>
  26. Chapman L, Magos A. Surgical and radiological management of uterine fibroids in the UK. *Curr Opin Obstet Gynecol* 2006; **18**: 394–401. doi: <https://doi.org/10.1097/01.gco.0000233933.13684.05>
  27. Park J-Y, Park S-K, Kim D-Y, Kim J-H, Kim Y-M, Kim Y-T, et al. The impact of tumor morcellation during surgery on the prognosis of patients with apparently early uterine leiomyosarcoma. *Gynecol Oncol* 2011; **122**: 255–9. doi: <https://doi.org/10.1016/j.ygyno.2011.04.021>
  28. Seidman MA, Oduyebo T, Muto MG, Crum CP, Nucci MR, Quade BJ. Peritoneal dissemination complicating morcellation of uterine mesenchymal neoplasms. *PLoS One* 2012; **7**: e50058. doi: <https://doi.org/10.1371/journal.pone.0050058>
  29. George S, Barysaukas C, Serrano C, Oduyebo T, Rauh-Hain JA, Del Carmen MG, et al. Retrospective cohort study evaluating the impact of intraperitoneal morcellation on outcomes of localized uterine leiomyosarcoma. *Cancer* 2014; **120**: 3154–8. doi: <https://doi.org/10.1002/cncr.28844>
  30. US Food and Drug Administration. *UPDATED—laparoscopic uterine power morcellation in hysterectomy and myomectomy: FDA safety communication*. Silver Spring: US Food and Drug Administration; 2014. <https://wayback.archive-it.org/7993/20170722215727/https://www.fda.gov/MedicalDevices/Safety/AlertsandNotices/ucm424443.htm>
  31. European Society for Gynaecological Endoscopy. SGE statement on morcellation. 2016. Available from: <https://esge.org/wp-content/uploads/2017/02/ESGE-Statement-on-Morcellation-02-May-2014.pdf>
  32. Kainsbak J, Hansen ES, Dueholm M. Literature review of outcomes and prevalence and case report of leiomyosarcomas and non-typical uterine smooth muscle leiomyoma tumors treated with uterine artery embolization. *Eur J Obstet Gynecol Reprod Biol* 2015; **191**: 130–7. doi: <https://doi.org/10.1016/j.ejogrb.2015.05.018>
  33. Whitaker L, Critchley HOD. Abnormal uterine bleeding. *Best Pract Res Clin Obstet Gynaecol* 2016; **34**: 54–65. doi: <https://doi.org/10.1016/j.bpobgyn.2015.11.012>
  34. Ueda H, Togashi K, Konishi I, Kataoka ML, Koyama T, Fujiwara T, et al. Unusual appearances of uterine leiomyomas: MR imaging findings and their histopathologic backgrounds. *Radiographics* 1999; **19 Spec No**: S131–45. doi: [https://doi.org/10.1148/radiographics.19.suppl\\_1.g99oc04s131](https://doi.org/10.1148/radiographics.19.suppl_1.g99oc04s131)
  35. Peng H-J, Zhao B, Yao Q-W, Qi H-T, Xu Z-D, Liu C. Intravenous leiomyomatosis: CT findings. *Abdom Imaging* 2012; **37**: 628–31. doi: <https://doi.org/10.1007/s00261-011-9798-6>
  36. Kocica MJ, Vranes MR, Kostic D, Kovacevic-Kostic N, Lackovic V, Bozic-Mihajlovic V, et al. Intravenous leiomyomatosis with extension to the heart: rare or underestimated? *J Thorac Cardiovasc Surg* 2005; **130**: 1724–6. doi: <https://doi.org/10.1016/j.jtcvs.2005.08.021>
  37. Andrade LA, Torresan RZ, Sales JF, Vicentini R, De Souza GA. Intravenous leiomyomatosis of the uterus. A report of three cases. *Pathol Oncol Res* 1998; **4**: 44–7. doi: <https://doi.org/10.1007/BF02904695>
  38. Evans AT, Symmonds RE, Gaffey TA. Recurrent pelvic intravenous leiomyomatosis. *Obstet Gynecol* 1981; **57**: 260–4.
  39. Shin MS, Fulmer JD, Ho KJ. Unusual computed tomographic manifestations of benign metastasizing leiomyomas as cavitary nodular lesions or interstitial lung disease. *Clin Imaging* 1996; **20**: 45–9. doi: [https://doi.org/10.1016/0899-7071\(94\)00076-X](https://doi.org/10.1016/0899-7071(94)00076-X)
  40. Fasih N, Prasad Shanbhogue AK, Macdonald DB, Fraser-Hill MA, Papadatos D, Kielar AZ, et al. Leiomyomas beyond the uterus: unusual locations, rare manifestations. *Radiographics* 2008; **28**: 1931–48. doi: <https://doi.org/10.1148/rg.287085095>
  41. Abramson S, Gilkeson RC, Goldstein JD, Woodard PK, Eisenberg R, Abramson N. Benign metastasizing leiomyoma: clinical, imaging, and pathologic correlation. *AJR Am J Roentgenol* 2001; **176**: 1409–13. doi: <https://doi.org/10.2214/ajr.176.6.1761409>
  42. Brown RS, Marley JL, Cassoni AM. Pseudo-Meigs' syndrome due to broad ligament leiomyoma: a mimic of metastatic ovarian carcinoma. *Clin Oncol* 1998; **10**: 198–201. doi: [https://doi.org/10.1016/S0936-6555\(98\)80071-X](https://doi.org/10.1016/S0936-6555(98)80071-X)
  43. Sala EJS, Atri M. Magnetic resonance imaging of benign adnexal disease. *Top Magn Reson Imaging* 2003; **14**: 305–27. doi: <https://doi.org/10.1097/00002142-200308000-00004>
  44. DeMulder D, Ascher SM. Uterine leiomyosarcoma: can MRI differentiate leiomyosarcoma from benign leiomyoma before treatment? *AJR Am J Roentgenol* 2018; **211**: 1405–15. doi: <https://doi.org/10.2214/AJR.17.19234>
  45. Zhao W-C, Bi F-F, Li D, Yang Q. Incidence and clinical characteristics of unexpected uterine sarcoma after hysterectomy and myomectomy for uterine fibroids: a retrospective study of 10,248 cases. *Onco Targets Ther* 2015; **8**: 2943–8. doi: <https://doi.org/10.2147/OTT.S92978>
  46. Wright JD, Tergas AI, Cui R, Burke WM, Hou JY, Ananth CV, et al. Use of electric power morcellation and prevalence of underlying cancer in women who undergo myomectomy. *JAMA Oncol* 2015; **1**: 69–77. doi: <https://doi.org/10.1001/jamaoncol.2014.206>

47. Parker WH, Fu YS, Berek JS. Uterine sarcoma in patients operated on for presumed leiomyoma and rapidly growing leiomyoma. *Obstet Gynecol* 1994; **83**: 414–8.
48. Sala E, Rockall AG, Freeman SJ, Mitchell DG, Reinhold C. The added role of Mr imaging in treatment stratification of patients with gynecologic malignancies: what the radiologist needs to know. *Radiology* 2013; **266**: 717–40. doi: <https://doi.org/10.1148/radiol.12120315>
49. Felix AS, Cook LS, Gaudet MM, Rohan TE, Schouten LJ, Setiawan VW, et al. The etiology of uterine sarcomas: a pooled analysis of the epidemiology of endometrial cancer Consortium. *Br J Cancer* 2013; **108**: 727–34. doi: <https://doi.org/10.1038/bjc.2013.2>
50. Harlow BL, Weiss NS, Lofton S. The epidemiology of sarcomas of the uterus. *J Natl Cancer Inst* 1986; **76**: 399–402.
51. Santos P, Cunha TM. Uterine sarcomas: clinical presentation and MRI features. *Diagn Interv Radiol* 2015; **21**: 4–9. doi: <https://doi.org/10.5152/dir.2014.14053>
52. Hayashi T, Horiuchi A, Sano K, Hiraoka N, Ichimura T, Sudo T, et al. Potential diagnostic biomarkers: differential expression of LMP2/β1i and cyclin B1 in human uterine leiomyosarcoma. *Tumori Journal* 2014; **100**: e99–106. doi: <https://doi.org/10.1177/1636.17918>
53. Danielson LS, Menendez S, Attolini CS-O, Guijarro MV, Bisogna M, Wei J, et al. A differentiation-based microRNA signature identifies leiomyosarcoma as a mesenchymal stem cell-related malignancy. *Am J Pathol* 2010; **177**: 908–17. doi: <https://doi.org/10.2353/ajpath.2010.091150>
54. Conklin CMJ, Longacre TA. Endometrial stromal tumors: the new who classification. *Adv Anat Pathol* 2014; **21**: 383–93. doi: <https://doi.org/10.1097/PAP.0000000000000046>
55. Tse KY, Crawford R, Ngan HYS. Staging of uterine sarcomas. *Best Pract Res Clin Obstet Gynaecol* 2011; **25**: 733–49. doi: <https://doi.org/10.1016/j.bpobgyn.2011.05.011>
56. D'Angelo E, Prat J. Uterine sarcomas: a review. *Gynecol Oncol* 2010; **116**: 131–9. doi: <https://doi.org/10.1016/j.ygyno.2009.09.023>
57. Pecorelli S. Revised FIGO staging for carcinoma of the vulva, cervix, and endometrium. *Int J Gynaecol Obstet* 2009; **105**: 103–4. doi: <https://doi.org/10.1016/j.ijgo.2009.02.012>
58. Koyama T, Togashi K, Konishi I, Kobayashi H, Ueda H, Kataoka ML, et al. Mr imaging of endometrial stromal sarcoma: correlation with pathologic findings. *AJR Am J Roentgenol* 1999; **173**: 767–72. doi: <https://doi.org/10.2214/ajr.173.3.10470920>
59. Ueda M, Otsuka M, Hatakenaka M, Sakai S, Ono M, Yoshimitsu K, et al. Mr imaging findings of uterine endometrial stromal sarcoma: differentiation from endometrial carcinoma. *Eur Radiol* 2001; **11**: 28–33. doi: <https://doi.org/10.1007/s003300000541>
60. Yoshizako T, Wada A, Kitagaki H, Ishikawa N, Miyazaki K. Mr imaging of uterine adenocarcinoma: case report and literature review. *Magn Reson Med Sci* 2011; **10**: 251–4. doi: <https://doi.org/10.2463/mrms.10.251>
61. Takeuchi M, Matsuzaki K, Nishitani H. Hyperintense uterine myometrial masses on T2-weighted magnetic resonance imaging: differentiation with diffusion-weighted magnetic resonance imaging. *J Comput Assist Tomogr* 2009; **33**: 834–7. doi: <https://doi.org/10.1097/RCT.0b013e318197ec6f>
62. Inoue A, Yamaguchi K, Kurata Y, Murakami R, Abiko K, Hamanishi J, et al. Unenhanced region on magnetic resonance imaging represents tumor progression in uterine carcinosarcoma. *J Gynecol Oncol* 2017; **28**: e62. doi: <https://doi.org/10.3802/jgo.2017.28.e62>
63. Gerges L, Popiolek D, Rosenkrantz AB. Explorative investigation of Whole-Lesion histogram MRI metrics for differentiating uterine leiomyomas and leiomyosarcomas. *AJR Am J Roentgenol* 2018; **210**: 1172–7. doi: <https://doi.org/10.2214/AJR.17.18605>
64. Nagai T, Takai Y, Akahori T, Ishida H, Hanaoka T, Uotani T, et al. Novel uterine sarcoma preoperative diagnosis score predicts the need for surgery in patients presenting with a uterine mass. *Springerplus* 2014; **3**: 678. doi: <https://doi.org/10.1186/2193-1801-3-678>
65. Kusunoki S, Terao Y, Ujihira T, Fujino K, Kaneda H, Kimura M, et al. Efficacy of PET/CT to exclude leiomyoma in patients with lesions suspicious for uterine sarcoma on MRI. *Taiwan J Obstet Gynecol* 2017; **56**: 508–13. doi: <https://doi.org/10.1016/j.tjog.2017.05.003>
66. Park JY, Lee JW, Lee HJ, Lee JJ, Moon SH, Kang SY, et al. Prognostic significance of preoperative <sup>18</sup>F-FDG PET/CT in uterine leiomyosarcoma. *J Gynecol Oncol* 2017; **28**: e28. doi: <https://doi.org/10.3802/jgo.2017.28.e28>
67. Lee HJ, Park J-Y, Lee JJ, Kim MH, Kim D-Y, Suh D-S, et al. Comparison of MRI and <sup>18</sup>F-FDG PET/CT in the preoperative evaluation of uterine carcinosarcoma. *Gynecol Oncol* 2016; **140**: 409–14. doi: <https://doi.org/10.1016/j.ygyno.2016.01.009>
68. Yamane T, Takaoka A, Kita M, Imai Y, Senda M. <sup>18</sup>F-FLT PET performs better than <sup>18</sup>F-FDG PET in differentiating malignant uterine corpus tumors from benign leiomyoma. *Ann Nucl Med* 2012; **26**: 478–84. doi: <https://doi.org/10.1007/s12149-012-0597-0>